Proceedings of the XVII ECSMGE-2019
Geotechnical Engineering foundation of the future
ISBN 978-9935-9436-1-3

doi: 10.32075/17ECSMGE-2019-0465

XVII European Conference
ECSMGE 2019
Reykjavik
on Soil Mechanics
and Geotechnical Engineering

Microstructure of compacted fly ash

Microstructure des cendres volantes compactées

K. Zabielska-Adamska
Bialystok University of Technology, Bialystok, Poland

D. Małaszkiewicz, M. Konopko
Bialystok University of Technology, Bialystok, Poland

ABSTRACT: Compacted fly ash from combustion of bituminous coal in conventional furnaces, despite its macroscopic similarity to non-cohesive soils, should always be evaluated considering moisture content at compaction, as in the case of compacted cohesive soils. The mechanical parameters and hydraulic conductivity of fly ash depend strictly on the moisture content at compaction. However, fly ash differs in structure from cohesive mineral soils. The microstructure studies were performed on samples of fly ash compacted according to the standard Proctor method of optimum water content ± 5%. The various microstructure of fly ash compacted at both sides of optimum water content was determined by means of ESEM image analysis.

RÉSUMÉ: Cendres volantes compactées provenant de la combustion de charbon bitumineux dans les fours conventionnels, malgré sa similitude macroscopique avec les sols non cohésifs, doivent toujours être évaluées en tenant compte de la teneur en humidité lors du compactage, comme dans le cas des sols cohésifs compactés. Les paramètres mécaniques et la conductivité hydraulique des cendres volantes dépendent strictement de la teneur en humidité lors du compactage. Cependant, la structure des cendres volantes diffère de celle des sols minéraux cohésifs. Les études de microstructure ont été effectuées sur des échantillons de cendres volantes compactées selon la méthode standard de Proctor avec une teneur en eau optimale ± 5%. La microstructure variée des cendres volantes compactées des deux côtés d'une teneur en eau optimale a été mise en évidence par analyse d'image ESEM.

Keywords: fly ash, microstructure, moisture content at compaction, propertes of compacted soil

1 INTRODUCTION

Fly ash is by-product of coal combustion in conventional power plants that is captured by electrostatic precipitators from exhaust gases. Fly ash particles are generally spherical in shape and range in size from about 1 to 100 µm. It is a heterogeneous material with very diverse mineral composition, mainly made of SiO_2, Al_2O_3, Fe_2O_3 and CaO, and with trace element concentrations generally similar to those in unpolluted soils.

Compacted fly ash from bituminous coal, despite its macroscopic similarity to non-cohesive soils, should always be evaluated taking into account moisture content at compaction, as in the case of compacted cohesive soils. Mechanical parameters and hydraulic conductivity of fly ash depend strictly on the moisture content at compaction (Zabielska-Adamska 2018, Zabielska-Adamska and Sulewska 2015).

The aim of the study is to show that microstructure of the compacted fly ash at both side of optimum water content is different, which can explain behaviour of compacted fly ash, although it varies from cohesive soils.

2 PROPERTIES OF COMPACTED SOILS

In some classical works in the field of soil mechanics (e.g. Mitchell et al. 1965, Lambe and Whitman 1969) the engineering properties of compacted cohesive soils were related to the compaction water content, which was explained by the dispersed microstructure of soil compacted on the wet side and flocculated microstructure of the soil compacted on the dry side of the Proctor compaction curve. Tatsuoka and Correia (2016) relate it to specific value of saturation degree, as a parameter close related to suction.

Mercury intrusion porosimetry tests for cohesive soils confirmed that the microstructure on the dry side of optimum water content was composed of aggregates with well-defined large macro-pores and the small pores inside the aggregates (Delage et al. 1996; Tarantino and De Col 2008, Romero 2013). The macro-pores are usually filled with continuous air and less continuous water; water there is in the small pores inside the aggregates. For material compacted on the wet side of the Proctor optimum water content, the initial bimodal pore size distribution depends heavily on the state of saturation during compaction (Delage et al. 1996). Cohesive soil compacted wet of optimum presents a dispersed structure with continuous water phase in the pores and air phase in mostly occluded state. The as-compacted structure is erased on saturation (Burton et al., 2015). Macropore space decreases as the water content or the compaction energy increases, whereas the micropore space remains unaltered by compaction. Comparing the behaviour of saturated soils under oedometric compression, it is possible to conclude that the aggregates remain even at high stresses (Otálvaro et al. 2015), which was stated for laterite soil. Ferber et al. (2009) during swelling observation state that the process leads to a micropores increase and a macropores decrease. According to Alonso et al. (2013), if water accesses to an initially compacted dry soil, the microstructure will be saturated first, because of the strong affinity between water and clay platelets. As soon as the microvoids in clay aggregates are saturated, any excess water will start to fill the macropores. The water partially filling the macropores will have a significant effect on the soil because the capillary effects will be exhibited just by the water forming menisci between aggregates and inert soil particles.

Delage (2010) and Otálvaro et al. (2015) also use SEM images for estimation of microstructure, where structure with inter-aggregate large pores were well visible.

3 THE MICROSTRUCTURE RESERCH

3.1 Material

All the tests were carried out on the basis of fly ash from hard coal burning in Bialystok Thermal-Electric Power Plant, stored at a dry storage yard. The tested fly ash corresponds in graining to sandy silt with a median particle diameter, D_{50}, of 0.06 mm. The specific surface of tested fly ash, measured by means of the methylene blue spot test, is 21.01 m^2/g. This value is comparable to the specific surface of kaolinite (Santamarina et al. 2002). The specific density, ρ_s, is 2.12 g/cm^3. X-ray diffraction patterns of the fly ash indicated basic mineralogical composition as quartz (SiO_2), mullite ($3Al_2O_3 \cdot 2SiO_2$) and calcite ($CaCO_3$). The grain-size distribution curve obtained for an average sample is presented in Figure 1.

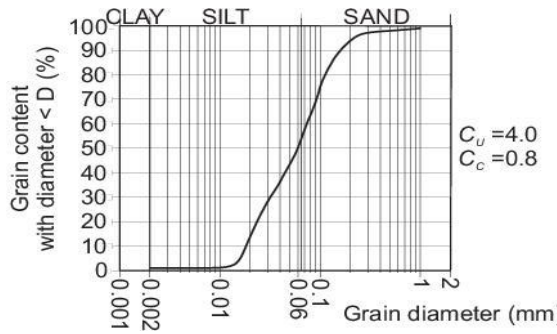

Figure 1. Grain-size distribution of tested fly ash

The microstructure tests were conducted to establish difference between structure of compacted fly ash at moisture content on both side of optimum water content, wet and dry side. So, the tested samples were compacted by the Standard Proctor at three different moisture contents within the range of w_{opt}±5%. Compaction curve is presented in Figure 2. Each point of the curve was determined for separately prepared sample because fly ash recompaction causes partial crumbling of dynamically rammed grains, which changes its compaction parameters (Zabielska-Adamska, 2008).

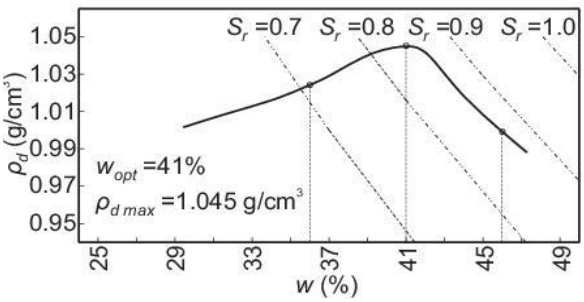

Figure 2. Compaction curve with marked points corresponding to the tested samples

3.2 Microstructure tests

Microstructural observations were performed using FEI Quanta 250 FEG Scanning Electron Microscope in ESEM mode. Because drying process could change the mictrostructure of material, the images were taken using gaseous SED (GSED) detector in ESEM mode that allows samples to be studied in their natural moisture content. The fly ash was tested directly after compaction. Samples were compacted in the oedometric ring to the density corresponding to the fly ash compaction curves. Their physical parameters are shown in Table 1. Structure was observed at natural breakthrough of the sample, without drying and coating.

It should be stated that mercury intrusion porosimetry tests (MIP), carried out in the case of cohesive soils for microstructure estimation, have not been prformed because of complete lack of plasticity of fly ash. Fly ash after drying, which is necessary to perform MIP analisys, does not preserve its structure, and behaves as non-cohesive soil.

Table 1. Tested sample parameters

Sample	w (%)	ρ_d (g/cm³)	n (–)	e (–)	S_r (–)
w_{opt} –5%	36	1.026	0.516	1.066	0.715
w_{opt}	41	1.045	0.507	1.029	0.844
w_{opt}+5%	46	1.001	0.528	1.118	0.872

3.3 The test results

Field of view analysed for each sample was about 550 μm in diameter (Fig. 3), chosen as representative for sample structure. Figures 4–6 present ESEM images of the fly ash samples compacted at different moisture content.

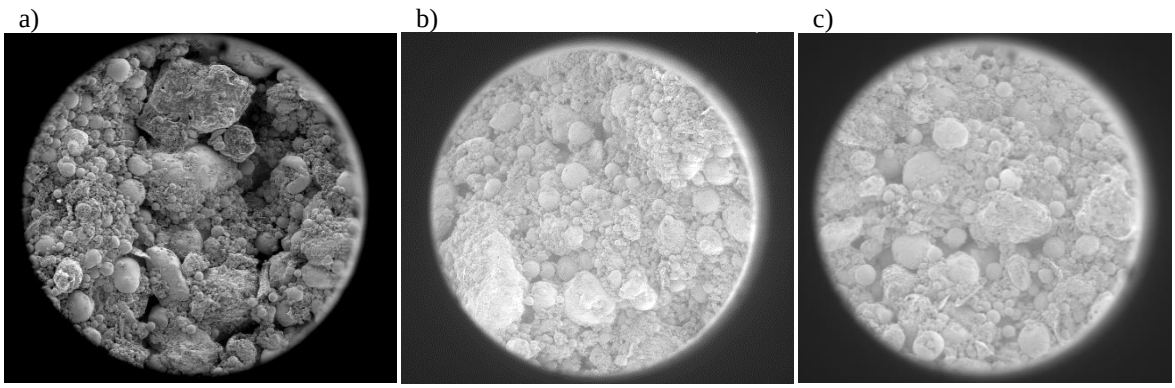

Figure 3. ESEM images of compacted fly ash (magn. 350x): a) w=36%, b) w=41%, c) w=46%

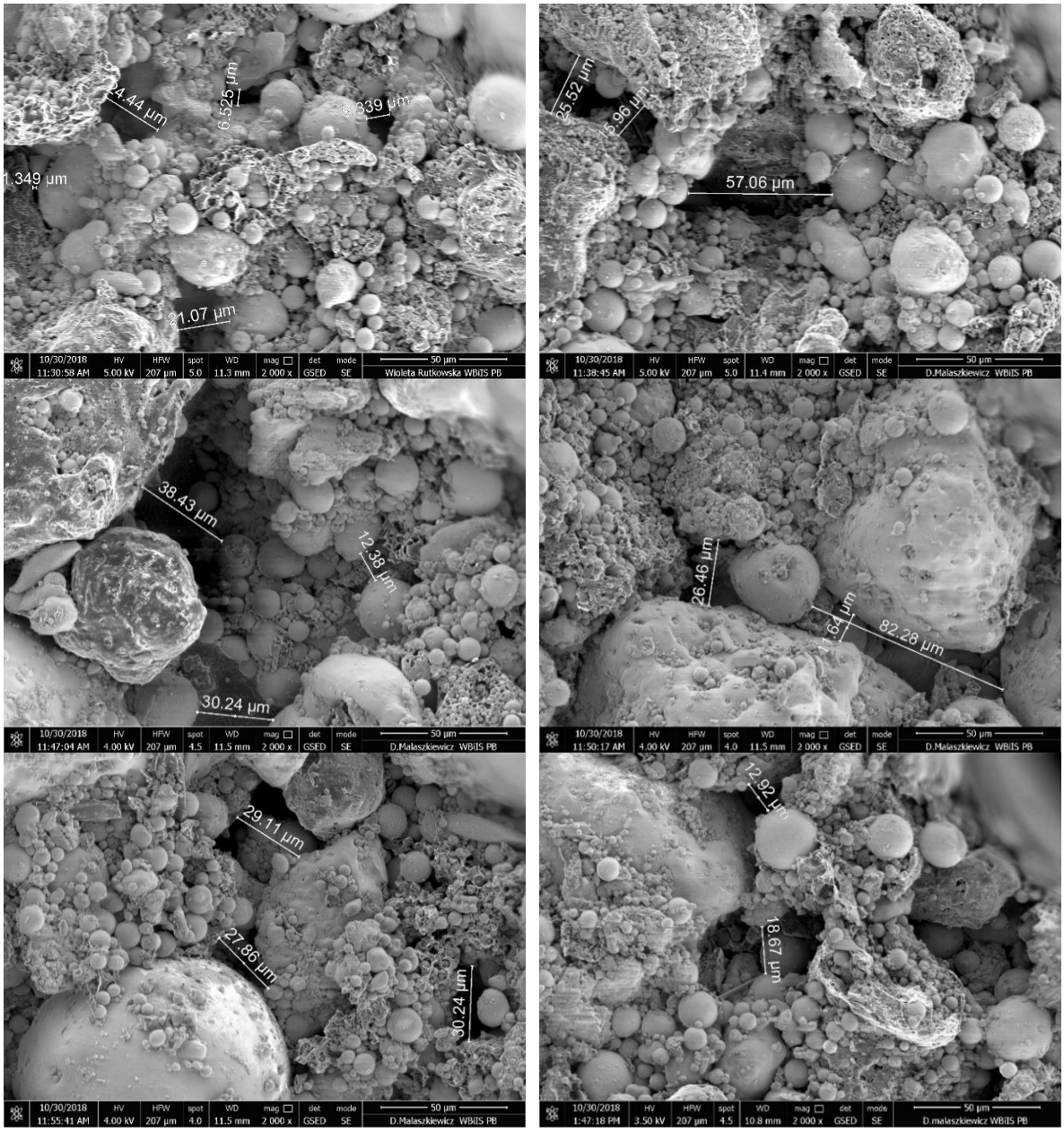

Figure 4. ESEM images of fly ash compacted at 36% ($w=w_{opt}$–5%)

Images were made with the same magnifiction of 2000x to enable the microstructure comparison. Samples compacted at water content ranging optimum water content, w_{opt}±5%, vary significantly. Sample compacted at the dry side of optimum water content (Fig. 4) is composed of aggregates, separated by pore spaces. The size of pore spaces range from 1.35 to 82.28 µm. Sample compacted at optimum water content is characterised by visibly tighter structure with

pore space ranged from 5.79 to 27.28 μm (Fig. 5) with the smallest number of pores. The structure of sample compacted at wet side of optimum is distinctly loose (Fig. 6), although the size of pore spaces does not differ significantly from sample at w_{opt} and it equals 1.21–27.28 μm. Porosity of the sample compacted at $w=w_{opt}+5\%$ is considerably greater in comparison to both other samples, so it must be a result of greater number of small pores between the particular particles. Figure 7 shows pore distribution histograms, and Figure 8 presents the statistical analysis of determined measurable pore space for all samples. It should be stated that median value, as the

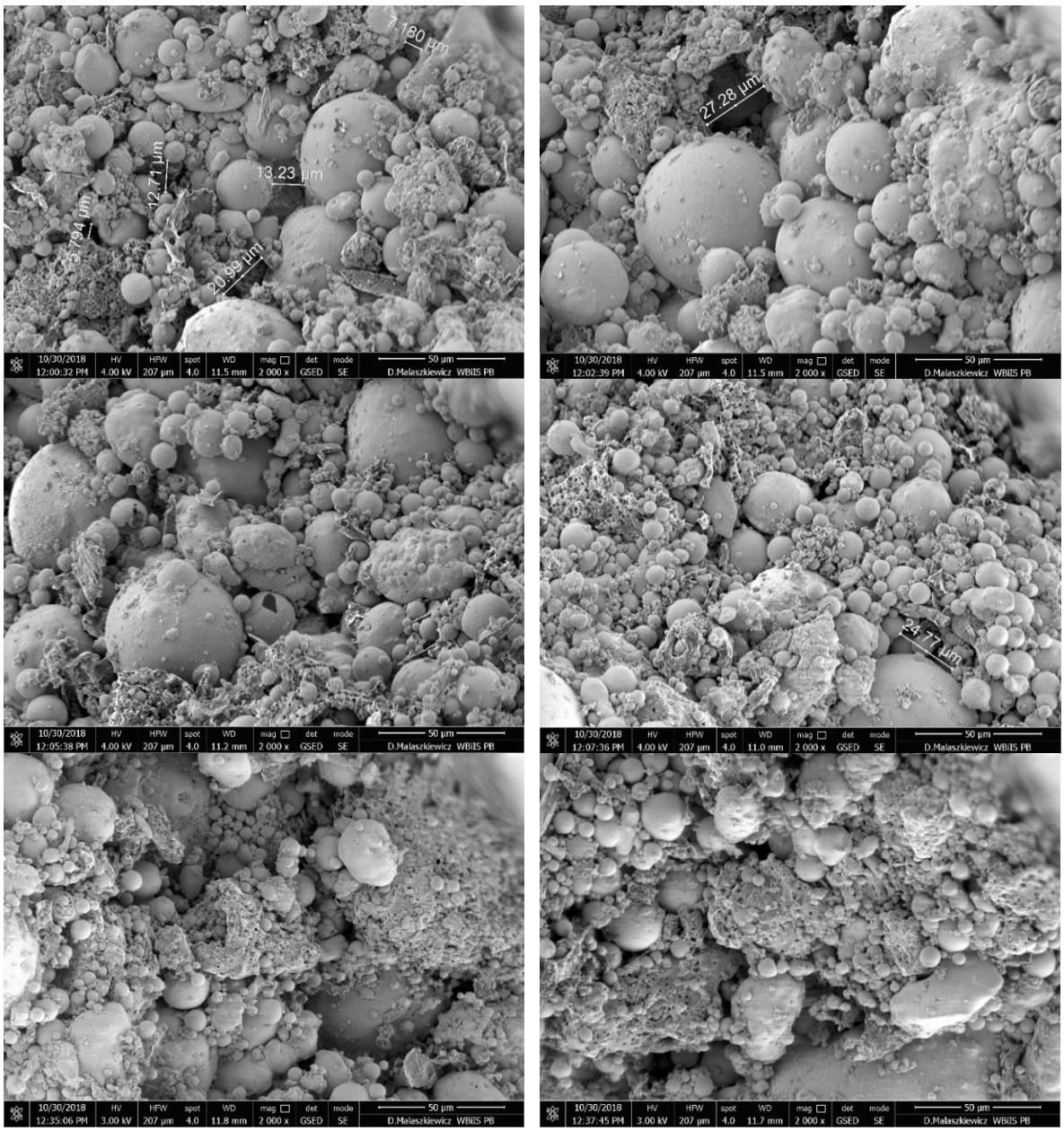

Figure 5. ESEM images of fly ash compacted at 41% ($w=w_{opt}$)

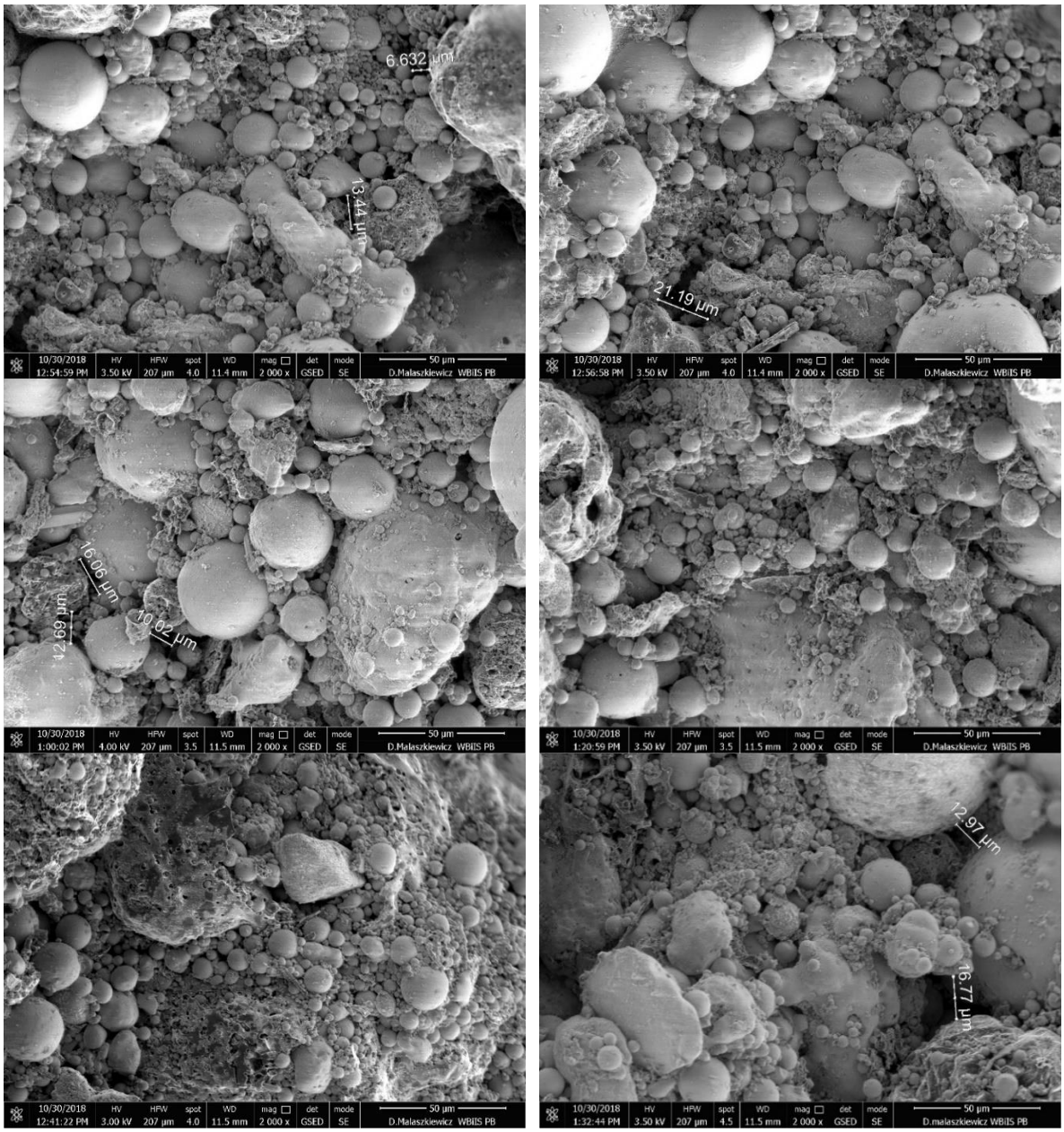

Figure 6. ESEM images of fly ash compacted at 46% ($w=w_{opt}+5\%$)

"middle" value, is better for pore size assesment than average value, which is especially visible in the case of sample compacted at $w \leq w_{opt}$, where the diverse individual pores can be observed. For sample with $w=w_{opt}-5\%$ average value of pore size is 25.34 µm and median value is 24.44 µm, and for $w=w_{opt}$ these values are equal to 13.68 µm and 12.71 µm, respectively.

The analysis of the Figure 7 suggests the multi-modal structure of fly ash samples compacted at or below optimum water content and

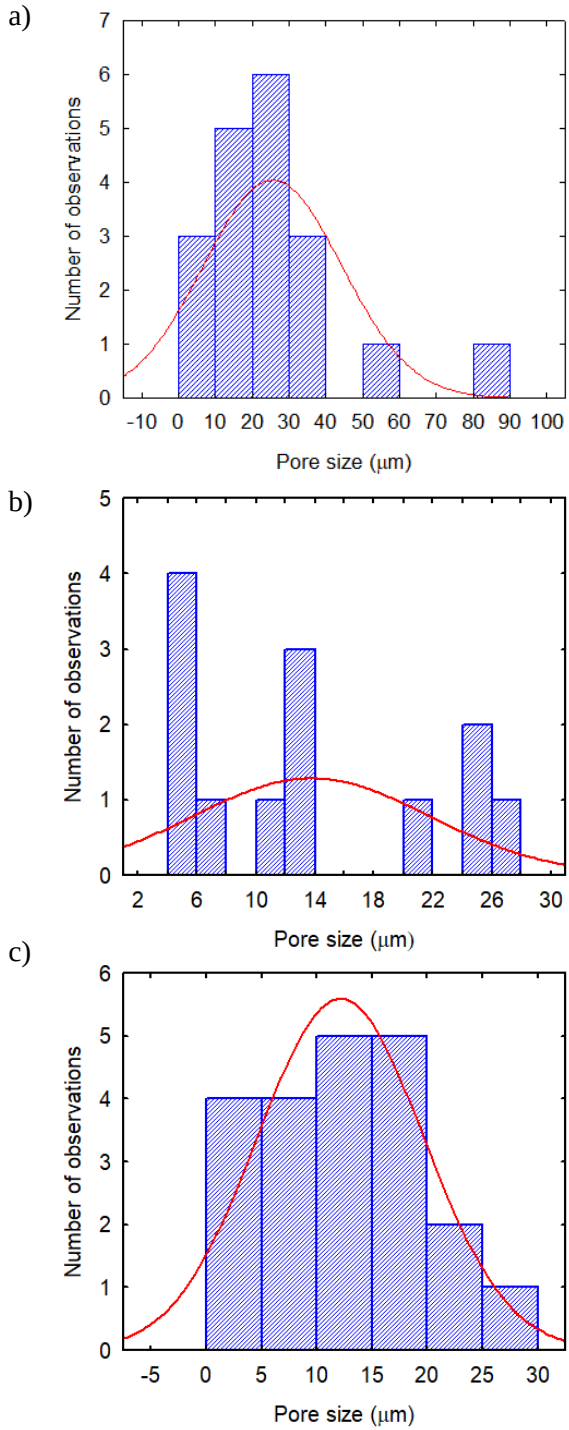

Figure 7. Pore size distribution: a) w_{opt}–5%, b) w_{opt}, c) w_{opt}+5%

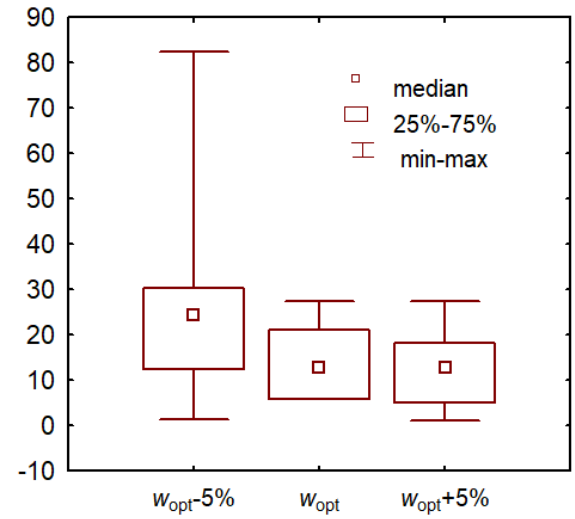

Figure 8. The statistical analysis of measurable pore space for the all samples

unimodal structure of samle compacted at wet side of optimum.

The ESEM image method should be considered rather a qualitative assessment, not a quantitative one.

4 CONCLUSIONS

The paper demonstrates the feasibility of using ESEM images to estimate the microstructure of compacted fly ash. Fly ash is non-cohesive, non-plastic material, so mercury intrusion porosimetry test can not be performed because of fly ash unstable structure after its drying.

The fly ash samples compacted at moisture content dry of optimum $w \leq w_{opt}$ show typical multi modal pore size distribution characteristics, whereas the fly ash samples compacted wet of optimum show typical unimodal pore size distribution characteristics.

The fly ash samples compacted at moisture content w=w_{opt}–5% show a structure composed of aggregates with well-defined large macro-pores and the small pores inside the aggregates, as in case of the cohesive soil.

Structure of sample compacted at optimum water content is the most uniform. Pore spaces are rather small, and they occur in small quantities.

In the case of sample compacted at $w=w_{opt}+5\%$ a great number of small pore spaces (measured and unmeasured) can be observed. It is visible that the fly ash structure is loosened by a higher water content during the compaction process.

5 ACKNOWLEDGEMENTS

This work, carried out in 2018 at the Bialystok University of Technology, was supported by Polish financial resources on science.

6 REFERENCES

Alonso, E.E., Pinyol, N.M. Gens, A. 2013. Compacted soil behaviour: initial state, structure and constitutive modelling, G*éotechnique* **63**, 463–478.

Burton, G.J., Pineda, J.A., Sheng, D., Airey, D. 2015. Microstructural changes of an undisturbed, reconstituted and compacted high plasticity clay subjected to wetting and drying. *Engineering Geology* **193**, 363–373.

Delage, P. 2010. A microstructure approach to the sensitivity and compressibility of some Eastern Canada sensitive clays, *Géotechnique* **60**, 353–368.

Delage, P., Audiguier, M., Cui, Y.J., Howat, M. 1996. Microstructure of a compacted silt, *Canadian Geotechnical Journal* **33**, 150–158.

Ferber, V., Auriol, J.C., Cui, Y.J., Magnan, J.P. 2009. On the swelling potential of compacted high plasticity clays, *Engineering Geology* **104**, 200–210.

Lambe, T.W., Whitman, R.V. 1969. *Soil Mechanics*, John Wiley & Sons, New York, USA.

Mitchell, J.K., Hooper, D.R., Campanella, R.G. 1965. Permeability of compacted clay, *Journal of Soil Mechanics and Foundation Division* **91**(SM4), 41–63.

Otálvaro, I.F., Neto, M.P.C., Caicedo, B. 2015. Compressibility and microstructure of compacted laterites, *Transportation Geotechnics* **5**, 20–34.

Romero, E. 2013. A microstructural insight into compacted clayey soils and their hydraulic properties, *Engineering Geology* **165**, 3–19.

Santamarina, J.C., Klein, K.A., Wang, Y.H., Prencke, E. 2002. Specific surface: determination and relevance, *Canadian Geotechnical Journal* **39**, 233–241.

Tarantino, A., De Col, E. 2008. Compaction behavior of clay, *Géotechnique* **58**, 199–213.

Tatsuoka, F., Correia, A.G. 2016. Importance of controlling the degree of saturation in soil compaction, Procedia Engineering 143, 556–565.

Zabielska-Adamska, K 2008. Laboratory compaction of fly ash and fly ash with cement additions, *Journal of Hazardous Materials* **151**, 481–489.

Zabielska-Adamska, K. 2018. One-dimensional compression and swelling of compacted fly ash, *Geotechnical Research* **5**, 96–105.

Zabielska-Adamska, K., Sulewska, M.J. 2015. Dynamic CBR test to assess the soil compaction, *Journal of Testing and Evaluation* **53**, 1028–1036.